Special issue of the 2nd International Conference on Computational and Experimental Science and Engineering (ICCESEN 2015)

Experimental and Numerical Determination of Casting-Mold Interfacial Heat Transfer Coefficient in the High Pressure Die Casting of A-360 Aluminum Alloy

M. Koru* and O. Serçe

Süleyman Demirel University, Energy Systems Engineering, Isparta, Turkey

Although die casting is a near net shape manufacturing process, it mainly involves a thermal process. Therefore, in order to produce high quality parts, it is important to determine casting-mold interfacial heat transfer coefficient and heat flux. In this paper the effects of different injection parameters (second phase velocity, injection pressure, pouring and die temperature) on heat flux and interfacial heat transfer coefficient were investigated experimentally and numerically. Experiments were performed in cylindrical geometry using a cast aluminum alloy A360 against H13 steel mold. Selected injection parameters were 1.7–2.5 m/s for second phase velocity, 100–200 bar for third phase pressure, 983–1053 K for pouring temperature and 373, 433, 493, 553 K for the die temperature. These parameters were used for both non-vacuum and vacuum conditions in the cavity of the mold. The effects of the application under vacuum conditions were also studied. Temperatures were measured as functions of time, using 18 thermocouples, which were mounted at different depths of casting and mold material. Measured and calculated temperature values are found compatible. Interfacial heat transfer coefficient h and heat flux q depending on the experimentally measured temperature values were calculated with finite difference method using explicit technique in C# programming language. In addition to experiments, Flow-3D software simulations were performed using the same parameters. Interfacial heat transfer coefficient and heat flux results obtained from Flow-3D are also presented in the study. Interfacial heat transfer coefficient has decreased as a result of increasing of temperature of mold and pouring. In addition, interfacial heat transfer coefficient values have increased slightly with the increase of injection speed and pressure. It was observed that the values of interfacial heat transfer coefficient and heat flux have also increased when vacuum was applied inside the cavity of the mold. When all injection parameters are considered, it is seen that the interfacial heat transfer coefficient varies between 92–117 kW/m^2 K.

DOI: 10.12693/APhysPolA.130.453

PACS/topics: 81.05.Bx, 47.11.Bc, 47.27.ek, 44.10.+i

1. Introduction

Nowadays aluminium materials are used widely in automotive industry due to their low density, high strength and thermal conductivity features. The most important method used in the manufacturing of aluminium parts is the high pressure die casting method which permits the direct production of the net shaped product. Due to the short cycle time in the high pressure die casting process (HPDC), the mold is exposed to large temperature fluctuations in each cycle. Therefore, the determination of the interfacial heat transfer coefficient (IHTC) in the HPDC process is extremely important. The heat transfer mechanism at the interface of mold and casting considerably affects the micro and macro structure of the casting component. Especially when HPDC is compared with other casting methods, the effect of high thermal conductivity of casting and mold material is important for the determination of IHTC [1–7].

The true determination of IHTC during the solidification in the HPDC process depends on the very precise determination of the thermodynamic properties of casting and mold material, which depend on temperature, distribution of mold temperature and boundary conditions. These parameters will vary depending on temperature and time throughout the process. During this process, while heat is transferred by conduction significantly, it also can be transferred by radiation and convection due to high temperature [6–10]. On the other hand, by the evacuation of the air in the mold cavity before the injection process, it is possible to improve interfacial contact between the casting and mold. Air evacuation system has been developed for this purpose. When the air in the mold cavity is discharged through the evacuation system, the amount of air voids at the interface of molten metal in contact with the mold will be decreased. In this case, the casting-mold IHTC is affected positively. In addition, literature results show that the mechanical properties of the samples are positively affected by application of vacuum [11–14].

In literature, there are two different methods used to determine the casting-mold IHTC. First on is based on the measurement of the interface gap size by the linear variable displacement transducer (LVDT) and determining of the IHTC depending on the gap size [15]. The other method is to measure the temperature with thermocouples placed at different points of the cast and mold material and to calculate the heat transfer coefficient of the interface by the numerical calculation methods (FDM, FEM).

This study aims to determine IHTC and heat flux according to different injection parameters (second phase velocity, injection pressure, pouring and die temperature,

*corresponding author; e-mail: muratkoru@sdu.edu.tr

vacuum and non-vacuum) of A360 aluminium alloy during HPDC. In this aspect, A360 aluminium alloy is used for casting material and H13 hot work steel is used for mold material. Numerical analysis is performed using Flow-3D simulation software for all injection parameters. The data obtained from the thermocouples placed in the casting and mold material, suitable for the cylindrical geometry, and the data obtained from the simulation software are treated by a computer code written in C# programming language depending on FDM to calculate the IHTC h and heat flux q values. The results obtained for the different injection parameters are compared with the literature values.

2. Materials and methods

2.1. Setting of experimental system

During the pressure casting process, a cylindrical geometry proper for standard tensile samples was made in a CAD software in order to determine the temperature distribution, heat flux and IHTC. The most appropriate gating and venting channels are designed using the casting simulation software. Resulting design is shown in Fig. 1.

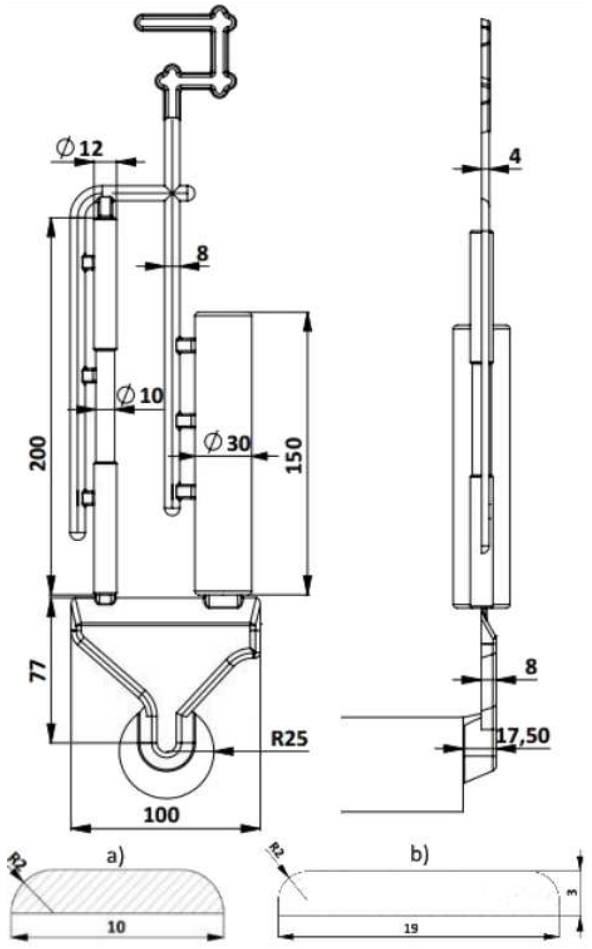

Fig. 1. The appearance of the parts, gating and vacuum channels used in experiments.

18 calibrated mineral insulated type-K thermocouples with ±1.5 °C measuring accuracy were placed radially in the cross section of the cylindrical part, in order to measure the temperature of the mold and of the A360 alloy (Fig. 2).

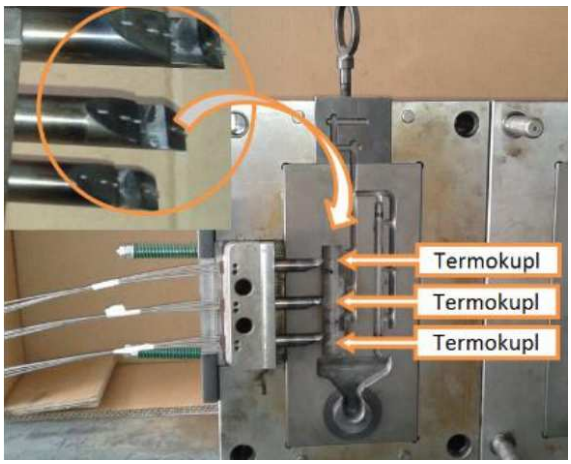

Fig. 2. Temperature measurement and thermocouple positioning.

TABLE I

Chemical composition of A360 alloy (wt.%).

Al	Si	Fe	Cu	Mg	Zn
77.4	9–10	1	0.6	0.4-0.6	0.4

In the experimental study of high pressure casting process, Al-Si alloy (A360) is used as cast alloy. The chemical composition of A360 alloy used in the experiments is given in Table I. Thermophysical properties of the mold and the casting material used in the experimental study are given in Table II [16].

TABLE II

Thermophysical properties of the mold and casting material.

Material	c [J/kg K]	ρ [kg/m^3]	k [W/mK]
H13	421.496+0.522T	7818.333–0.246T	25.174+0.008T
A360	963	2671.932–0.426T	113

The melting of casting material was made in the electric smelting furnace. Selected mold temperatures were 373, 433, 493, 553 K. Selected casting temperatures were 983 and 1053 K. The liquid metal was poured into the chamber of the pressure casting machine by means of a bucket. For pressure casting process, injection pressure (intensification pressure) was chosen as 100–200 bar and injection 2nd phase velocity was 1.7–2.5 m/s. In addition to these different parameters, the experiments were repeated using the vacuum device in vacuum and non-vacuum conditions.

During solidification, temperatures were measured using thermocouples in time interval of 0.004 seconds. These measured values have been recorded by a data acquisition unit (NI SCXI-1600) and have been transferred to a computer. Using this interface temperature set for mold and casting, IHTC and heat flux values were determined depending on the initial temperature of the mold.

2.2. Determination of time-dependent heat transfer coefficient with finite difference method

Due to the ease of application, the finite difference method (FDM) is used widely for finding numerical solutions. Using FDM a function is determined only at a number of discrete points. In such case, it is possible to estimate the value of the function in the other points. Because of this convenience, in many cases, the problem is reduced in the FDM. In Fig. 3, cylindrical coordinate system and application of the FDM are given.

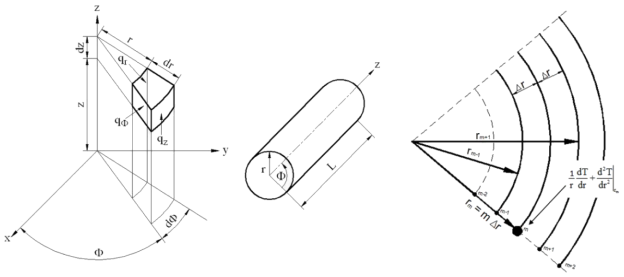

Fig. 3. The cylindrical coordinate system, differential control volume and the implementation of the FDM to the deriverative transactions.

The heat transfer coefficient h in the radial direction can be analyzed by Eq. (1) if mold and casting temperatures are differently chosen.

$$h = \frac{q}{(T_{\mathrm{C}} - T_{\mathrm{M}})} = \frac{\frac{1}{r}\frac{\partial}{\partial r}\left(kr\frac{\partial T}{\partial r}\right)}{(T_{\mathrm{C}} - T_{\mathrm{M}})}. \tag{1}$$

For solid and liquid phase conditions of both mold material and casting material, the solution of unidimensional time-dependent equation in cylindrical geometry, the heat transfer equation, is obtained as time-dependent temperature distribution

$$\rho c' \frac{\mathrm{d}T}{\mathrm{d}t} = \frac{1}{r}\frac{\mathrm{d}}{\mathrm{d}r}\left(kr\frac{\mathrm{d}T}{\mathrm{d}r}\right). \tag{2}$$

In Eq. (2), if k is independent of temperature, it is possible to write the right side of this equation as given in Eq. (3)

$$\frac{1}{r}\frac{\mathrm{d}}{\mathrm{d}r}\left(r\frac{\mathrm{d}T}{\mathrm{d}r}\right) = r\frac{d^2T}{\mathrm{d}r^2} + \frac{\mathrm{d}T}{\mathrm{d}r}. \tag{3}$$

After calculating the derivative of function $T(r)$, using the center of difference r_m point, Eq. (4) is obtained

$$\frac{1}{r}\frac{\mathrm{d}T(r)}{\mathrm{d}r} + \frac{\mathrm{d}^2T(r)}{\mathrm{d}r^2} = \frac{1}{(\Delta r)^2} \times \left\{\frac{1}{m}(T_{m+1} - T_{m-1}) + (T_{m-1} - 2T_m + T_{m+1})\right\}. \tag{4}$$

In FDM the reference point is generally named as node point and all these points are named as system. In this method, the sensitivity of the numerical solution is dependent on the number of determined system points. If the number of points is high, the solution is more sensitive. From this equation in cylindrical geometry, a suitable heat transfer equation for FDM calculation can be obtained as given in Eq. (5)

$$\frac{\rho c'}{k}\frac{\mathrm{d}T}{\mathrm{d}t} = \frac{1}{\alpha}\frac{\mathrm{d}T}{\mathrm{d}t} = \frac{1}{r}\frac{\mathrm{d}T}{\mathrm{d}r} + \frac{\mathrm{d}^2r}{\mathrm{d}r^2} \cong \frac{T_m^{t+\Delta t} - T_m^t}{\alpha\Delta t} = \frac{1}{m\Delta r}\frac{T_{m+1}^t - T_{m-1}^t}{2\Delta r} + \frac{T_{m-1}^t - 2T_m^t + T_{m+1}^t}{(\Delta r)^2}. \tag{5}$$

If Eq. (5) is used, $T_m^{t+\Delta t}$ term is obtained as given in Eq. (6). When Eq. (6) is arranged, Eq. (7) is obtained [17, 18]. In Eq. (8), T_m^t term must be larger than zero.

$$T_m^{t+\Delta t} = \frac{\alpha\Delta t}{(\Delta r)^2}\left\{\left[1 - \frac{\Delta r}{m\Delta r}\right]T_{m-1}^t + \left[1 + \frac{\Delta r}{m\Delta r}\right]T_{m-1}^t + \left[1 - \frac{\alpha\Delta t}{(\Delta r)^2}\right]T_m^t\right\} = F_0\left\{\left[1 - \frac{1}{m}\right]T_{m-1}^t + \left[1 + \frac{1}{m}\right]T_{m+1}^t\right\} + (1 - F_0)T_m^t \tag{6}$$

$$T_m^{t+\Delta t} = \frac{F_0}{r_m^2}\left\{\left[r_m - \frac{\Delta r}{2}\right]^2 T_{m-1}^t + \left[r_m + \frac{\Delta r}{2}\right]^2 T_{m+1}^t\right\} + \left\{1 - \frac{F_0}{r_m^2}\left[\left(r_m - \frac{\Delta r}{2}\right)^2 + \left(r_m + \frac{\Delta r}{2}\right)^2\right]\right\}T_m^t. \tag{7}$$

$$\frac{1}{F_0} \geq \frac{(r_m - \frac{\Delta r}{2})^2 + (r_m + \frac{\Delta r}{2})^2}{r_m^2}. \tag{8}$$

The temperatures measured by the thermocouples T_{M15}, located on the mold far away, 15 mm back of the interface, and T_{C15}, located on the casting far away, 15 mm from the interface, were used for the initial

boundary conditions. Measurements were used for determination of the other unknown temperatures of the nodes. Second boundary conditions were the temperature values taken from T_{C2} and T_{M2} thermocouples. The unknown temperatures were calculated by the Beck method. T_C and T_M were found for all time intervals and all nodes. Then, the IHTC h was calculated using Eq. (1).

2.3. Boundary conditions

As the initial boundary condition, the temperature values, measured by thermocouples, which were placed 15 mm behind and 15 mm in front of the mold interface, were used for all unknown temperatures of other nodes. At each time interval, the temperature of all nodes and interfaces in T_C and T_M were obtained.

3. Results and discussion

A total of 72 simulations were performed to investigate numerically the high pressure casting process. Simulations were performed using Flow-3D program. Solidification results obtained from the simulation program are shown in Fig. 4. In Fig. 4, it is seen that solidification starts at the thin wall portion of the tensile sample, near the vacuum valve. The last solidification area is located in the cylinder where the wall thickness is the largest.

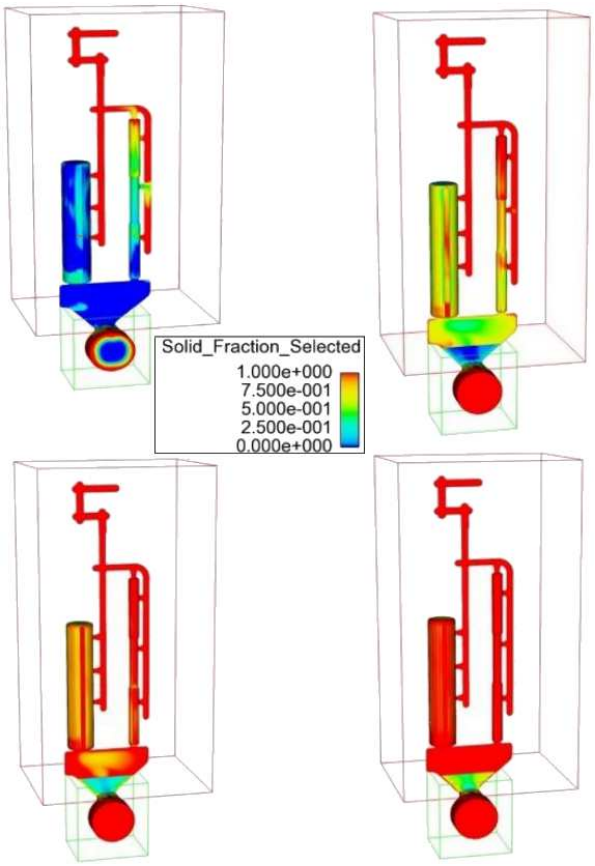

Fig. 4. The solidification simulation results from the simulation program.

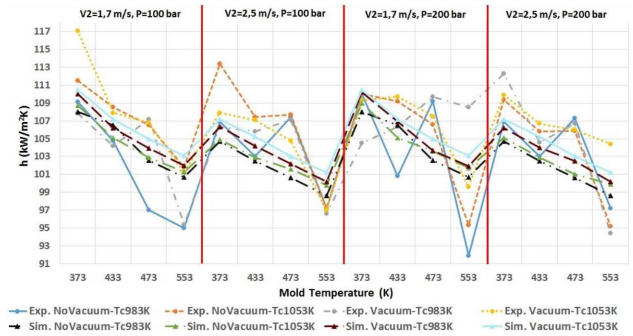

Fig. 5. IHTC results calculated from experimental results and taken from simulation (kW/m^2 K).

Figure 5 shows IHTC obtained by calculation using experiments and simulation program. Figure 6 presents the heat flux values for all parameters. When Fig. 5 is examined, it is seen that mold temperature has the highest effect on IHTC. By the increase of mold temperature, IHTC is reduced by 6% in both experimental and simulation results. Increasing the mold temperature reduces the value of heat flux by approximately 11% (Fig. 6). Srinivarsan [19], Dour [6] and Guo Zhi-Pengvd [20] have stated that increasing the mold temperature reduces IHTC. On the other hand, in studies of Hallam and Griffiths [16], IHTC has increased with the increase of mold temperature. When the casting is made at room temperature, IHTC values are 1700–2250 W/m^2 K, at mold temperature of 573 K these values are 1900–2080 W/m^2 K. Akar et al. [10] have determined that maximum IHTC at mold temperature of 373 K is 9749 W/m^2 K, at 423 K it is 14790 W/m^2 K and at 473 K it is 17300 W/m^2 K.

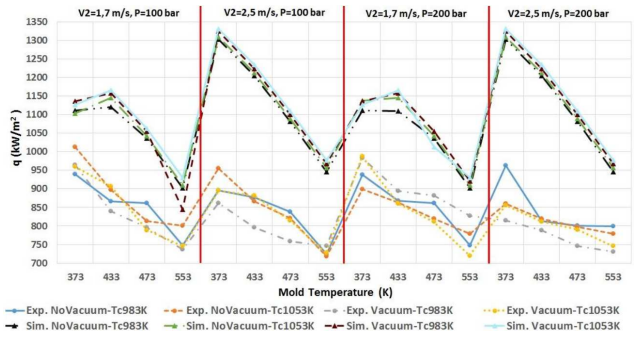

Fig. 6. Heat flux values calculated from experimental results and taken from simulations (kW/m^2).

Figures 5 and 6 show that when the casting temperature increases, IHTC and heat flux are increasing by 3% in experimental results and by 2% in simulation results. Kim et al. [3], have investigated casting temperature as function of mold-casting interfacial heat. Maximum IHTC value determined at casting temperature of 1033 K was 1360 W/m^2 K, at 1083 K it was 1640 W/m^2 K and at 1133 K it was 1860 W/m^2 K. They found that when the casting temperature was increased, the IHTC value had also increased.

Hamasaiid et al. [21] have investigated injection first and second phase velocities. When the injection velocity is increased, heat flux values are increased at both runner and body areas. Dour et al. [6] have investigated injection velocities and they stressed the important effect of velocities on heat flux. Similar to these studies, despite small change of velocity (1.7 to 2.5 m/s), when the injection velocity was increased, heat flux values have increased a little bit. Heat flux value is very high at the injection start value and then decreases gradually. Heat flux (5–20 kW/m^2) is increased with the increase of injection velocity. Dour et al. [6] have chosen 1.8–3.8 m/s in their study and as the result of study, the IHTC values are significantly increased with the increase of injection velocity.

When the injection pressure was increased from 100 bar to to 200 bar, IHTC value was increased by about 1–2 kW/m^2 K.

When Figs. 5 and 6 are analyzed in terms of vacuum application, one can see that heat flux and IHTC values are increased with vacuum application. This situation can be explained by the removal of air resistance. Since there is no resistance of air, mold-casting interfacial heat transfer effectively increases. However there is no big change in heat flux and IHTC values. With vacuum application heat flux value increases by about 10–20 kW/m^2 and IHTC value increases by about 3–5 kW/m^{2}K.

According to results of the study, expressions of the h and q values obtained by nonlinear regression method are presented below.

$$\begin{aligned} &h = a\mathrm{Vac} + bP + cV + dT_\mathrm{C} + eT_\mathrm{M} + f, \\ &a = -6.053125;\ b = 0.030718;\ c = -22.47265; \\ &d = -0.59049;\ e = -0.91380;\ f = 1911.92941. \end{aligned} \tag{9}$$

In the equation, h is heat transfer coefficient (kW/m^{2}K). Vac is vacuum application parameter. If vacuum is applied its value is 2, otherwise it is 1. P is injection pressure (bar), V is injection rate (m/s), T_C is casting temperature (K), T_M is mold temperature (K). The accuracy rate of this equation is 79%.

$$\begin{aligned} &q = a\mathrm{Vac} + bP + cV + dT_\mathrm{C} + eT_\mathrm{M} + f, \\ &a = 0.24687;\ b = -0.00665;\ c = 1.69921; \\ &d = 0.03129;\ e = -0.05686;\ f = 96.50668. \end{aligned} \tag{10}$$

In this equation, q is heat flux (kW/m^2) and the rest is the same as in Eq. (9). The accuracy rate of Eq. (10) is 59%.

4. Conclusions

- The temperature differences between experimental measurements and FLOW-3D simulation results are ranging from 5 to 25 K. This temperature difference reveals the eligibility of experimental temperature measurements.
- Experiments were repeated five times for the same experimental conditions. In addition, the difference between temperature values of these measurements is set at 10 K.
- Increase of the mold temperature reduces interfacial heat transfer coefficient and heat flux values. Eq. (1) reveals that heat flux value decreases when h value becomes stable with decreasing of the difference between casting and mold temperature. The results obtained from this study also support this. At the same time, Eq. (1) also reveals that heat flux and IHTC values decrease with respect to the increase of the mold temperature. Experimental results show similar outcomes.
- Increase of the casting temperature causes an increase in IHTC and also a decrease in heat flux.
- When the amount of air gap between the casting and the mold is reduced by vacuum application, IHTC is increased.
- Mold-casting IHTC and heat flux values can be calculated using Eqs. (9) and (10), which depend on the mold and casting temperatures as well as injection velocity, injection pressure and vacuum application parameters.
- When all injection parameters are considered, it is observed that the IHTC and heat flux change between 92–117 kW/m^2 K and 730–1320 kW/m^2, respectively.

Acknowledgments

This study was supported by the TUBİTAK the Scientific and Technological Research Council of Turkey, Project No: 114M003 and BAP Coordination Unit of the Süleyman Demirel University, Project No: 4416-YL1-15.

References

[1] H.H. Doehler, *Die Casting*, 1st ed., McGraw Hill, Michigan 1951, p. 502.

[2] C.M. Flemings, *Solidification Processing*, Mcgraw Hill College, New York 1974, p. 420.

[3] H.S. Kim, I.S. Cho, J.S. Shin, S.M. Lee, B.M. Moon, *ISIJ International* **45**, 192 (2005).

[4] J.E.Vinarcik, *High Integrity Die Casting Processes*, John Wiley & Sons, New York 2003, p. 223.

[5] B. Andersen, *Die casting engineering a hydraulic, thermal and mechanical process*, Marcel Dekker, New York 2005, p. 384.

[6] G. Dour, M. Dargusch, C. Davidson, A. Nef, *J. Mater. Proc. Technol.* **169**, 223 (2005).

[7] O. İpek, M. Koru, *J. Therm. Sci. Technol.* **31**, 45 (2011).

[8] Z.W. Chen, *Mater. Sci. Eng. A* **348**, 145 (2003).

[9] H.M. Şahin, K. Kocatepe, R. Kayıkçı, N. Akar, *Energ. Convers. Manag.* **47**, 19 (2006).

[10] N. Akar, H.M. Şahin, N. Yalçın, K. Kocatepe, *Exp. Heat Transfer* **21**, 83 (2008).

[11] B. Aksoylu, M.C. Ensari, *Metal Dünyası* **148**, 143 (2005).

[12] C.K. Jin, C.G. Kang, *J. Power Sources* **196**, 8241 (2011).

[13] C.K. Jin, C.G. Kang, *Int. J. Hydrogen En.* **32**, 1661 (2012).

[14] G.X. Wang, E.F. Matthys, *Int. J. Heat Mass Transfer* **45**, 4967 (2002).

[15] M. Trovant, Ph.D. Thesis, Graduate Department of Metallurgy and Materials Science, University of Toronto, 1998.

[16] C.P. Hallam, W.D. Griffiths, *Metall. Mater. Trans. B* **35**, 721 (2004).

[17] P.F. Incropera, D.P. Dewitt, *Heat and Mass Transfer Fundamentals*, Eds. T. Derbentli, O. Genceli, A. Güngör, A. Hepbaşlı, Z. İlken, N. Özbalta, F. Özgüç, C. Parmaksızoğlu, Y. Uralcan, Literatür Yayınları, İstanbul 2001, p. 960, (in Turkish).

[18] M.N. Özışık, *Finite difference methods in heat transfer*, Mechanical and Aerospace Engineering Department, North Carolina State University, Florida 1994, p. 412.

[19] M.N. Srinivasan, *Indian J. Technol.* **20**, 123 (1982).

[20] G. Zhi-Peng, X. Shou-Mei, L. Bai-Cheng, M. Lei, J. Allison, *Int. J. Heat Mass Transfer* **51**, 6032 (2008).

[21] A. Hamasaiid, G. Dour, M.S. Dargusch, T. Loulou, C. Davidson, G. Savage, *Metall. Mater. Trans. A* **39**, 853 (2008).